

Equilibrium and Heat of Adsorption for Organic Vapors and Activated Carbons

DAVID RAMIREZ, SHAOYING QI, AND MARK J. ROOD*

Department of Civil & Environmental Engineering,
205 North Mathews Avenue, University of Illinois at Urbana-Champaign, Urbana, Illinois 61801

K. JAMES HAY

U.S. Army Engineer Research and Development Center,
Construction Engineering Research Laboratory,
Champaign, Illinois 61826-9005

Determination of the adsorption properties of novel activated carbons is important to develop new air quality control technologies that can solve air quality problems in a more environmentally sustainable manner. Equilibrium adsorption capacities and heats of adsorption are important parameters for process analysis and design. Experimental adsorption isotherms were thus obtained for relevant organic vapors with activated carbon fiber cloth (ACFC) and coal-derived activated carbon adsorbents (CDAC). The Dubinin–Astakhov (DA) equation was used to describe the adsorption isotherms. The DA parameters were analytically and experimentally shown to be temperature independent. The resulting DA equations were used with the Clausius–Clapeyron equation to analytically determine the isosteric heat of adsorption (ΔH_s) of the adsorbate–adsorbent systems studied here. ACFC showed higher adsorption capacities for organic vapors than CDAC. ΔH_s values for the adsorbates were independent of the temperature for the conditions evaluated. ΔH_s values for acetone and benzene obtained in this study are comparable with values reported in the literature. This is the first time that ΔH_s values for organic vapors and these adsorbents are evaluated with an expression based on the Polanyi adsorption potential and the Clausius–Clapeyron equation.

Introduction

Microporous activated carbon adsorbents have been used extensively to remove a wide range of organic compounds from indoor air and industrial gas streams (1–4). Adsorption is accompanied by the transformations of energy, specifically during the sorption and desorption of the adsorbate. For example, Dombrowski et al. (5) determined that the heat of adsorption constitutes up to 30% of the electric energy consumed during regeneration of an adsorbent with an electrothermal-swing adsorption system. In addition, the temperature dependency of the equilibrium adsorption capacity is related directly to the heat of adsorption (6). Therefore, for process analysis and design, it is useful to know both the equilibrium adsorption capacities and isosteric heats of adsorption (ΔH_s) for relevant adsorbate–adsorbent systems.

* Corresponding author telephone: (217)333-6963; fax: (217)333-6968; e-mail: mrood@uiuc.edu.

This study evaluates the influence of equilibrium adsorption capacity and temperature on ΔH_s for two commercially available types of microporous activated carbons and two commonly used organic vapors. Equilibrium adsorption isotherms were experimentally determined at 101 kPa total pressure and between 20 and 50 °C. These results were then interpreted with data from the literature when describing the adsorption of benzene from 10 to 60 °C. The Dubinin–Astakhov (DA) equation, a commonly used isotherm model for physical adsorption of organic vapors onto microporous activated carbons, was then fitted and compared to the experimental data (7, 8). ΔH_s values were then determined using an analytical expression that was derived from the Clausius–Clapeyron and DA equations. The isotherms and ΔH_s values developed here are now available for subsequent design and optimization of air quality control adsorption systems.

Theoretical Background

DA Isotherm Equation. The DA equation was developed from the Polanyi concept of adsorption potential and adsorption characteristic curves. This equation relates the adsorption capacity (q) to the limiting adsorption capacity (q_0), the Polanyi adsorption potential (A), the characteristic energy of the adsorbent–adsorbate system (E), and the heterogeneity parameter (n) as described in eqs 1 and 2 (7, 9):

$$q = q_0 \exp\left[-\left(\frac{A}{E}\right)^n\right] \quad (1)$$

$$A = RT \ln \frac{P_0}{P} \quad (2)$$

where R is the universal gas constant, T is the equilibrium temperature, P_0 is the saturation vapor pressure, and P is the equilibrium bulk vapor pressure. The heterogeneity parameter is primarily determined by the adsorbent's pore dimension (9, 10). It has been shown that eq 1 can be derived from simple quantum mechanical assumptions (11) or statistical mechanical principles (12). In eq 1, q_0 is related to the limiting pore volume (W_0) by $q_0 = \rho W_0$, where ρ is the bulk density of condensed adsorbate. Equation 1 reduces to the Dubinin–Radushkevich (DR) equation when $n = 2$, which is widely used for organic vapor adsorbates and microporous activated carbon adsorbents (8, 12–14). To satisfy the temperature invariance of the Polanyi adsorption potential, the two DA parameters E and n must be independent of temperature (8).

Isosteric Heat with Polanyi Adsorption Potential. ΔH_s is one of the thermodynamic properties that are of special relevance to gas-phase adsorption systems (15). The Clausius–Clapeyron equation (6, 15–18), also known as the van't Hoff equation (2), expresses ΔH_s as

$$\Delta H_s = -R\left(\frac{\partial(\ln P)}{\partial(1/T)}\right)_q = RT^2\left(\frac{\partial(\ln P)}{\partial T}\right)_q \quad (3)$$

where ΔH_s is a function of both T and P at constant loading q . Substituting the Polanyi adsorption potential (eq 2) into the Clausius–Clapeyron equation of eq 3 yields:

$$\Delta H_s = \frac{RT^2}{P_0} \frac{dP_0}{dT} + A - T\left(\frac{\partial A}{\partial T}\right)_q \quad (4)$$

The first term to the right of the equal sign in eq 4 is the heat

Report Documentation Page			<i>Form Approved OMB No. 0704-0188</i>	
<p>Public reporting burden for the collection of information is estimated to average 1 hour per response, including the time for reviewing instructions, searching existing data sources, gathering and maintaining the data needed, and completing and reviewing the collection of information. Send comments regarding this burden estimate or any other aspect of this collection of information, including suggestions for reducing this burden, to Washington Headquarters Services, Directorate for Information Operations and Reports, 1215 Jefferson Davis Highway, Suite 1204, Arlington VA 22202-4302. Respondents should be aware that notwithstanding any other provision of law, no person shall be subject to a penalty for failing to comply with a collection of information if it does not display a currently valid OMB control number.</p>				
1. REPORT DATE 2005	2. REPORT TYPE	3. DATES COVERED 00-00-2005 to 00-00-2005		
4. TITLE AND SUBTITLE Equilibrium and Heat of Adsorption for Organic Vapors and Activated Carbons			5a. CONTRACT NUMBER	
			5b. GRANT NUMBER	
			5c. PROGRAM ELEMENT NUMBER	
6. AUTHOR(S)			5d. PROJECT NUMBER	
			5e. TASK NUMBER	
			5f. WORK UNIT NUMBER	
7. PERFORMING ORGANIZATION NAME(S) AND ADDRESS(ES) Department of Civil & Environmental Engineering, 205 North Mathews Avenue, University of Illinois at Urbana-Champaign, Urbana, IL, 61801			8. PERFORMING ORGANIZATION REPORT NUMBER	
9. SPONSORING/MONITORING AGENCY NAME(S) AND ADDRESS(ES)			10. SPONSOR/MONITOR'S ACRONYM(S)	
			11. SPONSOR/MONITOR'S REPORT NUMBER(S)	
12. DISTRIBUTION/AVAILABILITY STATEMENT Approved for public release; distribution unlimited				
13. SUPPLEMENTARY NOTES U.S. Government or Federal Rights.				
14. ABSTRACT				
15. SUBJECT TERMS				
16. SECURITY CLASSIFICATION OF:			17. LIMITATION OF ABSTRACT Same as Report (SAR)	18. NUMBER OF PAGES 8
a. REPORT unclassified	b. ABSTRACT unclassified	c. THIS PAGE unclassified		

of evaporation from a bulk liquid (2, 9). Given that P_0 is independent of the adsorbent, eqs 3 and 4 are identical. The partial derivative in eq 4 is then rewritten as (Appendix I):

$$\left(\frac{\partial A}{\partial T}\right)_q = \left(\frac{\partial A}{\partial T}\right)_\theta + \alpha \left(\frac{\partial A}{\partial \ln q}\right)_T \quad (5)$$

where α is the thermal coefficient of limiting adsorption defined by eq A-8 and θ is the pore filling or fractional surface loading defined as

$$\theta = \frac{q}{q_0} \quad (6)$$

Substituting eq 5 into eq 4 gives

$$\Delta H_s = \frac{RT^2}{P_0} \frac{dP_0}{dT} + A - T \left(\frac{\partial A}{\partial T}\right)_\theta - \alpha T \left(\frac{\partial A}{\partial \ln q}\right)_T \quad (7)$$

The derivation of ΔH_s from the Clausius–Clapeyron equation and the adsorption potential concept provides eq 7, which is identical to the general expression for the differential molar heat of adsorption developed from the Gibbs–Helmholtz equation by Bering and Serpinsky (9). However, this expression needs to be further evaluated so that it can be readily used to determine ΔH_s . For adsorption of select gases in micropores, there exists the characteristic curves of θ versus A that is independent of temperature (7, 9):

$$\left(\frac{\partial A}{\partial T}\right)_\theta = 0 \quad (8)$$

Substituting eq 8 into eq 7 yields

$$\Delta H_s = \frac{RT^2}{P_0} \frac{dP_0}{dT} + A - \alpha T \left(\frac{\partial A}{\partial \ln q}\right)_T \quad (9)$$

However, eq 9 still requires the evaluation of the partial derivative $(\partial A / \partial \ln q)_T$. The partial derivative can be evaluated if the adsorption isotherm or the relation between the vapor pressure and the surface loading is given explicitly. In the next section, this partial derivative is obtained from the DA equation for the adsorption isotherm and an expression for ΔH_s is obtained analytically.

Isosteric Heat with the DA Equation. ΔH_s can be expressed analytically from the Clausius–Clapeyron equation and using the DA equation for the equilibrium adsorption isotherm. Equation 1 is rewritten to express the adsorption potential as a function of surface loading:

$$A = E \left(\ln \frac{q_0}{q} \right)^{1/n} \quad (10)$$

Differentiating eq 10 with respect to q at constant temperature and substituting it into eq 9 gives the analytical relation between ΔH_s and pore filling (q/q_0) (2, 9):

$$\Delta H_s = \frac{RT^2}{P_0} \frac{dP_0}{dT} + E \left(\ln \frac{q_0}{q} \right)^{1/n} + \frac{\alpha TE}{n} \left(\ln \frac{q_0}{q} \right)^{1/n-1} \quad (11)$$

Equation 11 is the resulting ΔH_s equation that will be used with the experimental data. However, the values of α and dP_0/dT need to be evaluated. The evaluation of these physical parameters and further discussion about the limits of ΔH_s as q tends to 0 and q_0 are provided in Appendix II.

Experimental Apparatus and Procedure

Equilibrium adsorption capacities of acetone and benzene were determined using commercially available activated carbon fiber cloth (ACFC, ACFC-5092-20, American Kynol,

TABLE 1. Physical Properties of the Adsorbates Used in This Research (19)

adsorbate	T_c (K)	P_c (atm)	T_b (K)	ρ_b (g/cm ³)	ρ_c (g/cm ³)
acetone	508.1	46.38	329.2	0.735	0.517
benzene	562.2	48.26	353.2	0.813	0.654

Inc.) and coal-derived activated carbon (CDAC, BPL, Calgon Carbon Corporation). The ACFC is made from phenolic Novolac resin and has an N₂-BET surface area of 1604 m²/g and a narrow pore size distribution. The material is 95.4% pure carbon, with the balance consisting of H, O, and N. The ACFC is also ash-free to restrain unwanted chemical reactions that can occur with typical CDACs (20). CDAC used in this study has an N₂-BET surface area of 965 m²/g. CDAC has a large mass fraction of carbon, hydrogen, and oxygen and also contains ash and 1–4% by mass sulfur (21). Equilibrium adsorption isotherms and ΔH_s results are compared with results available in the literature that also use CDAC (22).

Adsorption isotherms were measured for adsorbate concentrations ranging from 0 to 196 000 ppmv (relative pressures from 0 to 0.8) for acetone and from 0 to 94 000 ppmv (relative pressures from 0 to 0.95) for benzene (Table 1). Temperature for the samples was controlled between 20 and 50 °C. The experimental apparatus was operated in a controlled temperature and humidity room ($T = 20$ °C, RH = 40%). The experiments involved passing the gaseous adsorbates of known concentration through a sample of adsorbent suspended in a gravimetric balance.

The experimental apparatus consisted of a gas generation system and a gravimetric balance. In the gas generation unit, liquid acetone or benzene (reagent grade) was supplied at a constant rate with a syringe (Hamilton 10 mL) and a syringe pump (kdScientific, model 100) and then mixed with ultra-high-purity (UHP) nitrogen. The UHP nitrogen was initially passed through a Drierite gas drier/purifier (containing anhydrous CaSO₄) in order to remove moisture and other contaminants from the gas stream before it was mixed with the organic vapor.

Mass flow controllers (Tylan, models FC-280, FC-260, and RO-28) were used to control the flow rates of the calibration and purge gas streams. N₂ flow rates were calibrated with a gas flow meter (Bios Drycal, model DC-2). The experimental temperatures were measured with a thermocouple (Omega, Type K) and controlled with an electrical heating tape and a Variac.

A gravimetric balance (Cahn Inc., model C-2000) was used to measure the changes in weight of the adsorbents during the adsorption of the adsorbates. Sample masses and gas temperatures were recorded with a computerized data acquisition system (Metrabyte, model DASH-08/EXP-16).

Before each run, the balance was zeroed and calibrated. The adsorbent sample was then placed on a sample pan and its initial weight was measured. The heating system was turned on, and the Variac setting was adjusted in order to increase the sample temperature to 165 °C for 30 min. There was no further observed change in weight of the sample after 30 min of treatment ($\Delta m / \Delta t < 2 \mu\text{g}/30 \text{ min}$). The detection limit of the sample weight for the gravimetric balance is 0.002 mg. Initial heating of the sample desorbed volatile contaminants from the adsorbent that had adsorbed during sample storage and handling. The heating system was then turned off and the sample was cooled to room temperature. The dry weight of the adsorbent was determined using the recorder zero suppression feature on the gravimetric balance. A dry flow of 200 mL/min N₂ was maintained through the sample chamber during zeroing, calibration, initial weight measurements, and subsequent experiments. This was done in order to offset any effects that the flowing gas stream could

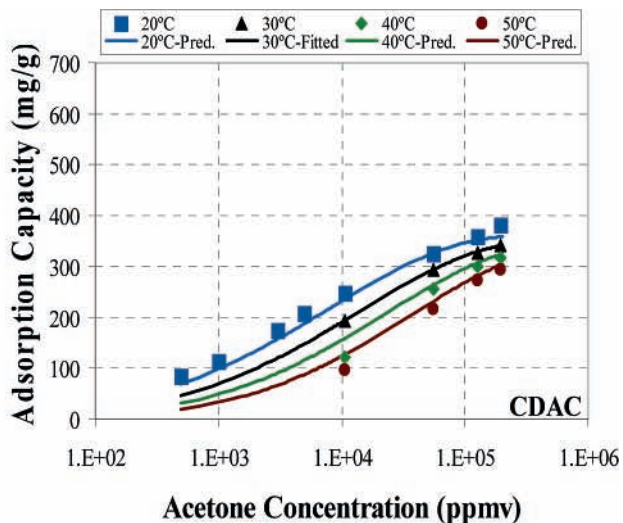
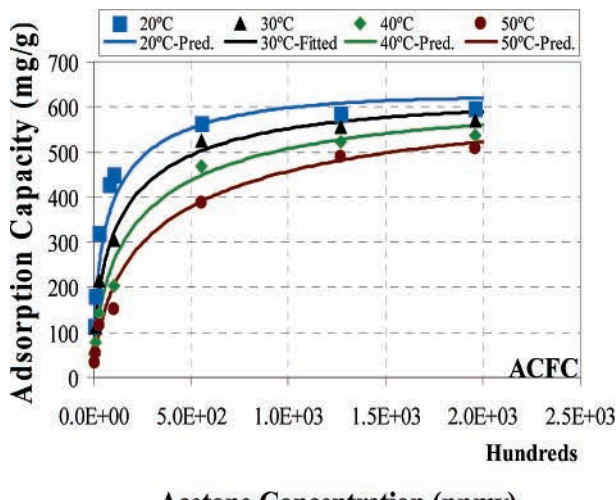


FIGURE 1. Adsorption capacities that were measured and then fitted or predicted with the DR equation for acetone with ACFC (linear axis) and CDAC (log x-axis) at selected temperatures. Experimental results are provided as symbols, while the fitted and predicted results are provided as lines.

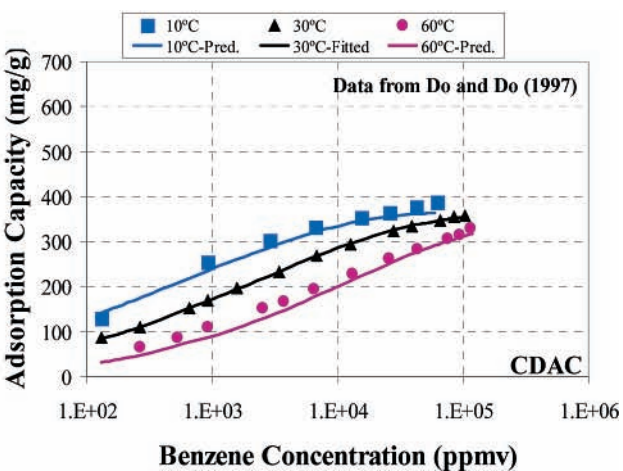
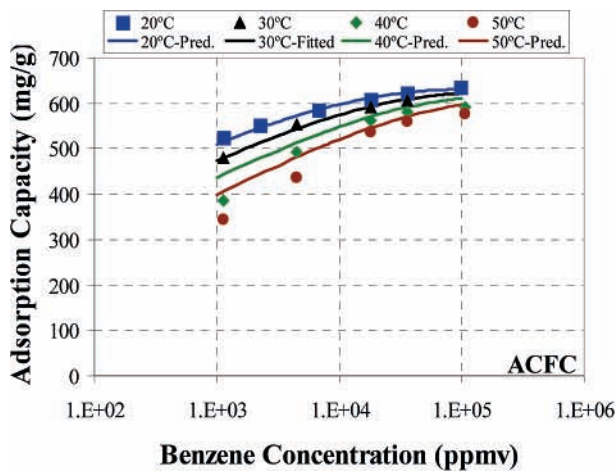


FIGURE 2. Adsorption capacities that were measured and then fitted or predicted with the DR equation for benzene with ACFC and CDAC at selected temperatures. Experimental results are provided as symbols, while the fitted and predicted results are provided as lines.

have due to the drag force on the sample pan. In addition, the N_2 flow prevented the adsorbent from adsorbing any moisture or other contaminants from the ambient air during the desorption and cooling steps. The N_2 flow also prevented any contamination of the electronics in the gravimetric balance.

The initial conditions for each adsorption capacity test were achieved by setting the N_2 flow to 200 mL/min and turning on the heating system to provide the desired experimental temperature to within ± 1 °C. The increase in the adsorbent weight was assumed to be due to adsorption of adsorbate and was monitored and recorded using a data acquisition system. The gas stream was kept flowing until no further change in weight was observed. The sample weight was then zeroed electronically, and the resulting weight gain was recorded. These steps were repeated for all gas stream's relative pressures and temperatures tested.

Results and Discussion

Adsorption Isotherms. Equilibrium adsorption isotherms for acetone and benzene adsorbates with ACFC and CDAC adsorbents in the range of 20–60 °C and at 101 kPa total pressure are provided in Figures 1 and 2. The adsorption capacities of the ACFC sample are 68–120% larger than the adsorption capacities of the CDAC sample at 30 °C as the

relative pressures of acetone and benzene approach one, respectively (Table 2). Such result is consistent with the bulk liquid densities of the adsorbates and the W_0 values of ACFC and CDAC of 0.726 and 0.522 cm³/g, respectively (21). A total of 55% of ACFC's and CDAC's adsorption capacities for acetone are utilized as acetone's concentration increases to 10 000 ppmv at 30 °C (Figure 1). In contrast, more than 80% of ACFC's and CDAC's adsorption capacities are utilized for benzene at the same vapor concentration and temperature (Figure 2). Benzene clearly adsorbed more effectively than acetone for both adsorbents due to its lower saturation vapor pressure and higher boiling point. ACFC's adsorption capacity for both adsorbates at 10 000 ppmv is larger than the total adsorption capacity for CDAC. ACFC's enhanced adsorption capacities at lower vapor concentrations is important because most air quality control applications that utilize physical adsorption as the mechanism to remove vapors from gas streams have vapor concentrations <10 000 ppmv. The lowest gas-phase concentration tested when generating the isotherms was 500 ppmv due to limitations with the instrumentation and carrier gas quality. However, the trend in results at lower gas-phase concentrations is expected to be similar as described here, with adsorption capacities decreasing with further reductions in gas-phase concentrations.

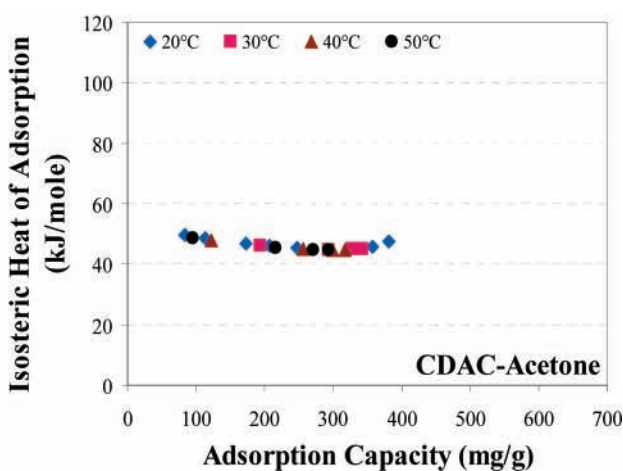
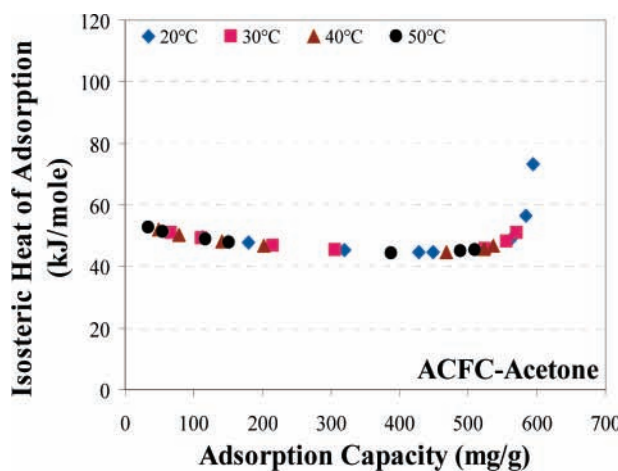


FIGURE 3. Isosteric heats of adsorption for ACFC–acetone and CDAC–acetone systems at selected temperatures.

TABLE 2. Adsorption Capacity Data for the Adsorbents and Adsorbates Studied

adsorbent	adsorbate	concn (ppmv)	adsorption capacity (mg of adsorbate/g of adsorbent)			
			20 °C	30 °C	40 °C	50 °C
ACFC	acetone	0	0	0	0	0
		500	113	67	49	34
		1 000	179	112	78	55
		3 000	320	215	141	117
		7 941	428	na ^a	na	na
		10 589	450	306	202	151
		55 595	562	524	468	388
		127 076	585	556	523	489
		195 909	595	570	537	509
		0	0	0	0	0
benzene	benzene	1 127	525	479	386	343
		2 255	552	na	na	na
		4 511	na	554	492	435
		6 767	585	na	na	na
		18 046	607	591	563	536
		36 092	622	606	581	561
		98 000	634	na	na	na
		106 022	na	na	591	576
		0	0	0	0	0
		500	84	na	na	na
CDAC	acetone	1 000	113	na	na	na
		3 000	173	na	na	na
		5 000	207	na	na	na
		10 589	247	194	122	95
		55 595	325	293	257	215
		127 076	358	328	299	272
		195 909	381	343	318	293

^a na, not available.

Increasing the adsorption temperature from 20 to 60 °C reduced the adsorption capacities of ACFC and CDAC by 20–60% for acetone and benzene, which indicates that physical adsorption is the mechanism causing the partitioning of the vapor between the gas and adsorbed phases. This temperature effect on the adsorption capacity is substantial at vapor concentrations <10 000 ppmv, which is important for air quality control applications.

As previously mentioned, ACFC and CDAC are primarily microporous activated carbon adsorbents. Hence, the DR equation ($n = 2$ in eq 1) was chosen to model the adsorption isotherms. The DR equation was initially fitted using isotherm data at 30 °C for each adsorbent–adsorbate system to determine E and W_0 (Table 3). Modeling the adsorption isotherms with the DR equation at 30 °C resulted in excellent fits with all of the regression coefficients (R^2) > 0.98. The DR equation was then used with the resulting E and W_0 values

TABLE 3. Isotherm Parameters for ACFC and CDAC

adsorbate	ACFC		CDAC		
	E (kJ/mol)	n	E (kJ/mol)	n	W_0 (cm ³ /g)
acetone	11.40	2	0.785	2	0.454 ^a
benzene	24.25	2	0.720	2	0.410 ^b

^a CDAC Calgon BPL. ^b CDAC (22).

TABLE 4. Thermal Coefficient of Limiting Adsorption and Heat of Evaporation from Bulk Fluid for Acetone and Benzene

adsorbate	thermal coeff of limiting adsorption (K ⁻¹)	heat of evaporation (kJ/mol)	heat of evaporation (kJ/mol; 23)
		acetone	benzene
acetone	0.00197	31.5	31.97
benzene	0.00104	33.8	34.09

to predict the adsorption isotherms at 10–60 °C (Figures 1 and 2). The temperature invariance of the DR parameter (E) given by eq B-5 is thus confirmed experimentally with all of the R^2 values >0.98 when comparing the predicted and measured adsorption isotherm results. This result is important because it allows the use of the DR equation without introducing any additional parameters to describe the temperature effect on adsorption isotherms for acetone and benzene in a dynamic model over the temperature range studied here.

Isosteric Heat of Adsorption. The magnitude and variability of ΔH_s for the adsorbent–adsorbate systems studied here were determined using eq 11. However, values for α and the heat of evaporation from bulk fluid are needed to calculate ΔH_s . These parameters were determined using eqs B-6 and B-8, respectively (Table 4). Note that the modeled heat of evaporation values are within 1.5% of the reported values provided in the literature. These values with the DR parameters (E and $n = 2$) and q/q_0 values, which were determined directly from the experimental isotherms, were also used as inputs for eq 11.

The dependence of ΔH_s on the adsorbent–adsorbate system, temperature, and surface loading is provided in Figures 3 and 4. The values of ΔH_s for all four systems increase with decreasing adsorbate loadings <200 mg/g and increase with increasing loadings >500 and >300 mg/g for ACFC and CDAC adsorbents, respectively. There is also a local minimum in ΔH_s values at intermediate loadings. Such trends are consistent with the limits set by eqs B-1 and B-2 (Table 5). Higher ΔH_s values at adsorbate loadings <200 mg/g suggest

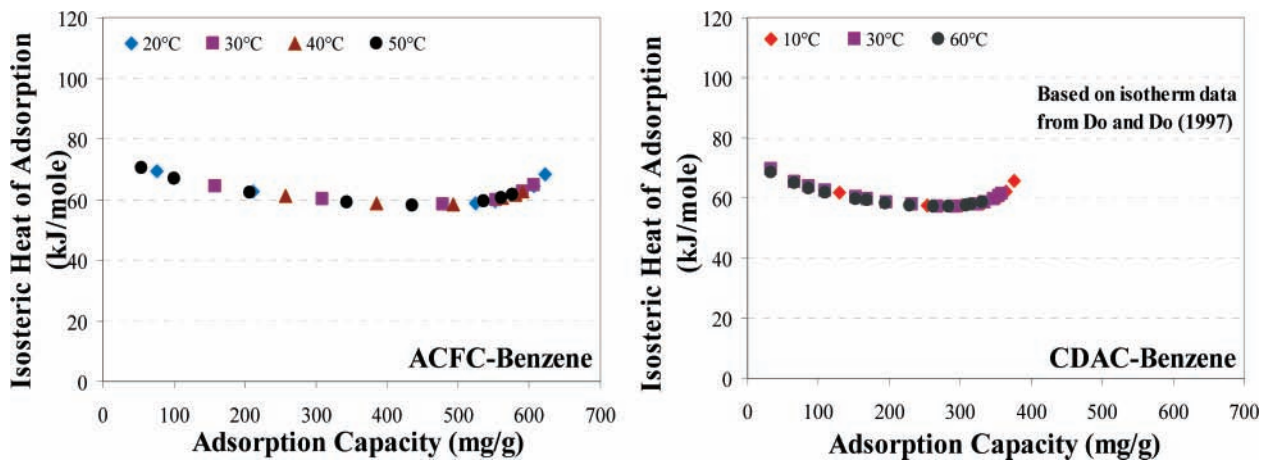


FIGURE 4. Isosteric heats of adsorption of ACFC–benzene and CDAC–benzene systems at selected temperatures.

TABLE 5. ΔH_s Data for the Adsorbents and Adsorbates in This Study

ACFC						CDAC					
acetone			benzene			acetone			benzene		
T (°C)	q (mg/g)	ΔH_s (kJ/mol)	T (°C)	q (mg/g)	ΔH_s (kJ/mol)	T (°C)	q (mg/g)	ΔH_s (kJ/mol)	T (°C)	q (mg/g)	ΔH_s (kJ/mol)
20	113	49.50	20	76	70.17	20	84	49.75	10	129	61.85
	179	47.74		211	63.39		113	48.59		254	57.64
	320	45.46		525	59.40		173	46.84		303	57.42
	428	44.68		552	60.33		207	46.13		332	58.30
	450	44.68		585	62.87		247	45.47		354	60.17
	562	48.93		607	66.50		325	45.08		364	61.97
	585	56.34		622	71.46		358	45.79		375	65.57
	595	73.24		158	65.15		381	47.43		33	69.49
	67	51.10	30	309	60.57	30	194	46.18	30	129	61.85
	112	49.28		479	58.81		293	44.90		254	57.64
30	215	46.79		554	60.59		328	45.01		303	57.42
	306	45.43		591	63.95		343	45.27		332	58.30
	524	45.85		606	66.67		122	47.83		354	60.17
	556	48.20	40	257	61.64		257	45.04		364	61.97
	570	50.78		386	59.19		299	44.79		375	65.57
40	49	51.84		492	58.95	40	318	44.85	40	129	61.85
	78	50.31		563	61.34		95	48.59		254	57.64
	141	48.21		581	62.98		215	45.47		303	57.42
	202	46.83		591	64.26		272	44.80		332	58.30
	468	44.60	50	55	71.23		293	44.71		354	60.17
	523	45.83		101	67.60		318	44.85		364	61.97
	537	46.61		207	62.96		215	45.47		375	65.57
	34	52.76		343	59.72	50	95	48.59	50	129	61.85
	55	51.26		435	58.78		215	45.47		254	57.64
50	117	48.70		536	60.10		272	44.80		303	57.42
	151	47.76		561	61.43		293	44.71		332	58.30
	388	44.44		576	62.74		318	44.85		354	60.17
	489	44.84					95	48.59		364	61.97
	509	45.35					215	45.47		375	65.57
							272	44.80		332	58.30
							293	44.71		354	60.17
							318	44.85		364	61.97
							95	48.59		375	65.57
							215	45.47		332	58.30

stronger interactions of the adsorbate with available surface functional groups located on the surface of the adsorbent. For example, about 10% of the ACFC's functional groups correspond to the oxygen containing alcohol group (20, 24). Stronger interactions between acetone vapor, which has a large dipole moment, and these oxygen containing surface functional sites is a plausible reason for the increasing ΔH_s values with decreasing vapor concentrations and adsorbate loadings at low adsorbate loadings (25). In contrast, increasing values of ΔH_s at adsorbate loadings >500 mg/g can be attributed to stronger lateral interactions of the adsorbates'

molecular aggregates that might be formed inside the adsorbents' micropores. The trend in Figures 3 and 4, which describe the increase in ΔH_s values with increasing equilibrium adsorption capacities at large adsorbate loadings, is similar to the trend reported in the literature for the adsorption of SO_2 on pitch-based activated carbon fiber. Such trend was attributed to strong lateral adsorbate interactions (25). The value of ΔH_s also approaches a minimum value at intermediate values of surface loading for all four systems. Such property can be further considered by analyzing the first and the second partial derivatives of ΔH_s with respect

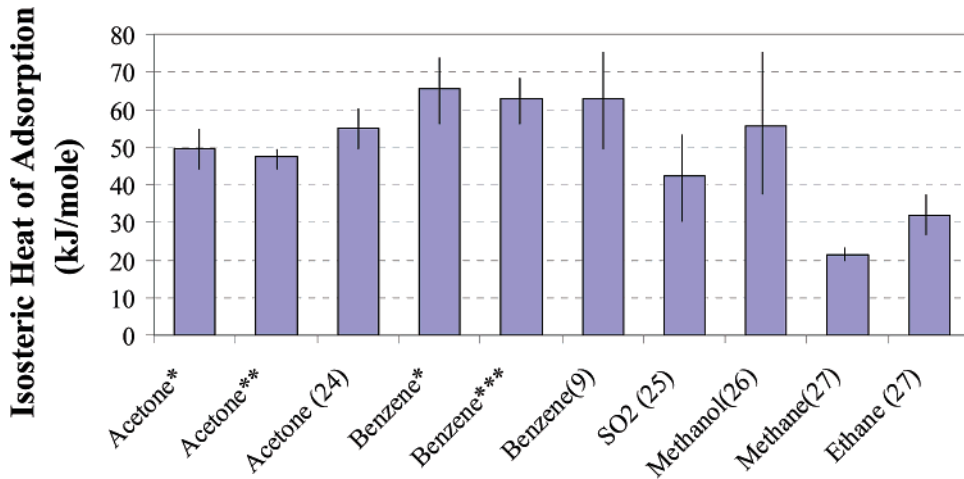


FIGURE 5. Comparison of ΔH_s values in this study with ΔH_s values available in the literature. (*) ACFC, this study; (**) CDAC, this study; (***) CDAC (22).

to the surface loading at constant temperature using eq 11. Appendix III provides a detailed mathematical development of the first and second partial derivatives of eq 11 that proves the existence of a minimum value for ΔH_s .

The resulting values for ΔH_s for all four systems remain relatively constant and as the relative surface loading (q/q_0) for acetone and benzene ranged from 6×10^{-4} to 0.8 and from 3×10^{-5} to 0.95, respectively (Figures 3 and 4). ΔH_s values varied from 44 to 55 kJ/mol for acetone and from 57 to 74 kJ/mol for benzene. ΔH_s values for acetone that were determined in this study are consistent with the values determined using the thermal equation of equilibrium adsorption and Clausius–Clapeyron equation for acetone (25). Literature values for ΔH_s ranged from 50 to 75 kJ/mol when studying the adsorption of acetone (25) and benzene (9) vapors. Calorimetric measurements of ΔH_s for SO₂ (30–55 kJ/mol; 26), for methanol (35–76 kJ/mol; 27), and for methane and ethane (20–38 kJ/mol; 28) are of the same order of magnitude as the results reported here for adsorption of acetone and benzene (Figure 5).

Values of the corresponding net heat of adsorption, obtained by subtracting the heat of evaporation from bulk fluid from the isosteric heat of adsorption, are 12.5–23.5 kJ/mol for acetone and 23.2–40.2 kJ/mol for benzene. Therefore, the heat of evaporation from the bulk fluid is the main contributing factor to ΔH_s for both acetone and benzene at these surface loadings.

Isosteric heat of adsorption values based on the adsorption isotherm data at four different temperatures agreed with each other as shown for acetone and benzene (Figures 3 and 4). These results confirm that ΔH_s values for both adsorbates are independent of temperature for the conditions studied here.

Acknowledgments

This research is supported by the Construction Engineering Research Laboratory (USACERL). CONACYT-Mexico support is also acknowledged.

Appendix I: Derivation of Equation 5

For a given adsorbent and adsorbate system, the general adsorption isotherm may be written as (9)

$$f(q, A, T) = 0 \quad (A-1)$$

or

$$g(\theta, A, T) = 0 \quad (A-2)$$

Differentiating eqs A-1 and A-2 gives, respectively:

$$\left(\frac{\partial q}{\partial A}\right)_T \left(\frac{\partial T}{\partial q}\right)_A \left(\frac{\partial A}{\partial T}\right)_q = -1 \quad (A-3)$$

and

$$\left(\frac{\partial \theta}{\partial A}\right)_T \left(\frac{\partial T}{\partial \theta}\right)_A \left(\frac{\partial A}{\partial T}\right)_{\theta} = -1 \quad (A-4)$$

If q_0 is a function of temperature alone, then the first partial derivative in eq A-3 is evaluated to give

$$\left(\frac{\partial q}{\partial A}\right)_T = \left(\frac{\partial(q_0 \theta)}{\partial A}\right)_T = q_0 \left(\frac{\partial \theta}{\partial A}\right)_T \quad (A-5)$$

Since q depends on both T and $\theta = q/q_0$, the second partial derivative in eq A-3 is rewritten as

$$\left(\frac{\partial T}{\partial q}\right)_A = \left(\frac{\partial T}{\partial \theta}\right)_A \left(\frac{\partial \theta}{\partial q}\right)_A \quad (A-6)$$

where

$$\begin{aligned} \left(\frac{\partial \theta}{\partial q}\right)_A &= \left(\frac{\partial(q/q_0)}{\partial q}\right)_A = \frac{1}{q_0} + \frac{q}{q_0} \left(-\frac{1}{q_0} \frac{\partial q_0}{\partial T} \frac{\partial T}{\partial q}\right)_A = \\ &\quad \frac{1}{q_0} + \alpha \frac{q}{q_0} \left(\frac{\partial T}{\partial q}\right)_A \end{aligned} \quad (A-7)$$

and

$$\alpha = -\frac{1}{q_0} \left(\frac{\partial q_0}{\partial T}\right)_A \quad (A-8)$$

Substituting eq A-7 into eq A-6 gives

$$\left(\frac{\partial T}{\partial q}\right)_A = \left(\frac{1}{q_0} + \alpha \frac{q}{q_0} \left(\frac{\partial T}{\partial q}\right)_A\right) \left(\frac{\partial T}{\partial \theta}\right)_A \quad (A-9)$$

Substituting eqs A-6 and A-9 into eq A-3 gives

$$\left(1 + \alpha q \left(\frac{\partial T}{\partial q}\right)_A\right) \left(\frac{\partial T}{\partial \theta}\right)_A \left(\frac{\partial \theta}{\partial A}\right)_T \left(\frac{\partial A}{\partial T}\right)_q = -1 \quad (A-10)$$

Combining eqs A-4 and A-10 leads to the following expression:

$$\left(\frac{\partial A}{\partial T}\right)_q + \alpha q \left(\frac{\partial T}{\partial q}\right)_A \left(\frac{\partial A}{\partial T}\right)_q = \left(\frac{\partial A}{\partial T}\right)_\theta \quad (\text{A-11})$$

Equation A-3 is rewritten to give

$$\left(\frac{\partial T}{\partial q}\right)_A \left(\frac{\partial A}{\partial T}\right)_q = -\left(\frac{\partial A}{\partial q}\right)_T \quad (\text{A-12})$$

Subsequently, substituting eq A-12 into eq A-11 yields eq 5.

Appendix II: Examining the Limits of the ΔH_s Equation

The first term to the right of the equal sign in eq 11 is the heat of evaporation from a bulk liquid, and the sum of the second and third terms is the net heat of adsorption (2, 9). The net heat of adsorption determines the surface loading dependency of ΔH_s . With the increase in surface loading, the contribution from the second term decreases while the contribution from the third term increases. For $n > 1$, ΔH_s is infinite at either zero or saturation surface loading since:

$$\lim_{q \rightarrow 0} \Delta H_s \rightarrow \lim_{q \rightarrow 0} \left[E \left(\ln \frac{q_0}{q} \right)^{1/n} \right] \rightarrow \infty \quad (n > 1, T = \text{constant}) \quad (\text{B-1})$$

$$\lim_{q \rightarrow q_0} \Delta H_s \rightarrow \lim_{q \rightarrow q_0} \left[\frac{\alpha TE}{n} \left(\ln \frac{q_0}{q} \right)^{1/n-1} \right] \rightarrow \infty \quad (n > 1, T = \text{constant}) \quad (\text{B-2})$$

As previously mentioned, both DA isotherm parameters n and E are independent of temperature because of the temperature invariance of adsorption potential given by eq 8. This can be readily proved by first rewriting eq 1 to express the equilibrium vapor pressure as a function of surface loading:

$$\ln P = \ln P_0 - \frac{E}{RT} \left(\ln \frac{q_0}{q} \right)^{1/n} \quad (\text{B-3})$$

At constant surface loading, differentiating eq B-3 gives

$$\begin{aligned} \left(\frac{\partial \ln P}{\partial T} \right)_q &= \frac{1}{P_0} \frac{dP_0}{dT} + \frac{E}{RT^2} \left(\ln \frac{q_0}{q} \right)^{1/n} - \\ &\quad \frac{E}{nRT} \frac{1}{q_0} \frac{dq_0}{dT} \left(\ln \frac{q_0}{q} \right)^{1/n-1} - \frac{1}{RT} \left(\ln \frac{q_0}{q} \right)^{1/n} \frac{dE}{dT} + \\ &\quad \frac{E}{RT} \left[\ln \left(\ln \frac{q_0}{q} \right) \right] \left(\ln \frac{q_0}{q} \right)^{1/n} \frac{1}{n^2} \frac{dn}{dT} \end{aligned} \quad (\text{B-4})$$

Subsequently substituting eqs A-8 and B-4 into eq 3 yields

$$\begin{aligned} \Delta H_s &= \frac{RT^2}{P_0} \frac{dP_0}{dT} + E \left(\ln \frac{q_0}{q} \right)^{1/n} + \frac{\alpha TE}{n} \left(\ln \frac{q_0}{q} \right)^{1/n-1} - \\ &\quad T \left(\ln \frac{q_0}{q} \right)^{1/n} \frac{dE}{dT} + ET \left[\ln \left(\ln \frac{q_0}{q} \right) \right] \left(\ln \frac{q_0}{q} \right)^{1/n} \frac{1}{n^2} \frac{dn}{dT} \end{aligned} \quad (\text{B-5})$$

Both eqs 11 and B-5 are derived from the same Clausius–Clapeyron equation to describe ΔH_s . Equation 11 is based on the temperature invariance of the Polanyi adsorption potential of eq 8, while no assumption is used regarding the temperature dependence of E and n during the derivation of eq B-5. Setting eqs B-1 and B-5 equal and comparing the terms involved thus suggests both E and n are independent of temperature.

Physical Parameters. Input parameters to describe the isotherm and ΔH_s are E and n , the thermal coefficient of limiting adsorption (α), the saturated vapor pressure (P_0), and the bulk vapor pressure (P). Parameters E and n are determined using the nonlinear regression analysis of

experimental isotherm data at a given temperature. Determination of the remaining parameters is provided below.

Assuming that the limiting pore volume (W_0) is independent of temperature, α is expressed analytically as (2)

$$\alpha = -\frac{\int_{\rho_b}^{\rho_c} \frac{d[\ln(W_0 \rho)]}{dT}}{\int_{T_b}^{T_c} dT} = \frac{1}{T_c - T_b} \ln \left(\frac{\rho_b}{\rho_c} \right) \quad (\text{B-6})$$

where ρ_b and ρ_c are the densities at the normal boiling temperature (T_b) and at the critical temperature (T_c), respectively (9, 19).

P_0 can be computed for a variety of organic vapors using the Wagner equation (19):

$$P_0 = P_c \exp \left(\frac{a_1 x + a_2 x^{1.5} + a_3 x^3 + a_4 x^6}{1 - x} \right) \left(\frac{760.0}{1.013} \right) \quad (\text{B-7})$$

where $x = (1 - T/T_c)$ and a_1 – a_4 are constants for a given adsorbate. Values for T_c , P_c , and a_1 – a_4 are available in the literature (19). Differentiating eq B-7 results in the following equation that expresses the heat of evaporation from bulk liquid as

$$\begin{aligned} \frac{RT^2}{P_0} \frac{dP_0}{dT} &= \\ \frac{RT^2}{T_c} \left(\frac{-a_1 - 1.5a_2 x^{0.5} + 0.5a_2 x^{1.5} - 3a_3 x^2 + 2a_3 x^3 - 6a_4 x^5 + 5a_4 x^6}{(1 - x)^2} \right) \end{aligned} \quad (\text{B-8})$$

Temperature Invariance of E and n . Comparing eqs 11 and B-5 results that

$$-T \left(\ln \frac{q_0}{q} \right)^{1/n} \frac{dE}{dT} + ET \left[\ln \left(\ln \frac{q_0}{q} \right) \right] \left(\ln \frac{q_0}{q} \right)^{1/n} \frac{1}{n^2} \frac{dn}{dT} = 0 \quad (\text{B-9})$$

Since the coefficients are nonzero, eq B-9 is simplified to

$$\frac{1}{E} \frac{dE}{dT} - \left[\ln \left(\ln \frac{q_0}{q} \right) \right] \frac{1}{n^2} \frac{dn}{dT} = 0 \quad (\text{B-10})$$

One solution to eq B-10 is the following:

$$\frac{dE}{dT} = 0 \text{ and } \frac{dn}{dT} = 0 \quad (\text{B-11})$$

In fact, eq B-11 is the only solution to eq B-10. By examining eq B-10, one may notice that for $dE/dT = 0$, dn/dT has to be zero, and for $dn/dT = 0$, dE/dT has to be zero. If there were any non-zero values for both dE/dT and dn/dT , eq B-10 could be rearranged to give

$$d \left(\ln E \right) - \left[\ln \left(\ln \frac{q_0}{q} \right) \right] \frac{1}{n^2} dn = 0 \quad (\text{B-12})$$

Integrating eq B-12 would lead to the following equation:

$$\ln E + \frac{1}{n} \left[\ln \left(\ln \frac{q_0}{q} \right) \right] = \text{constant} \quad (\text{B-13})$$

Equation B-13 suggests that for a given n , E would vary with the surface loading. This result contradicts the fact that both n and E are independent of surface loading; therefore, the

hypothesis of the existence of any non-zero values for both dE/dT and dn/dT is invalid.

Appendix III: First and Second Partial Derivatives of Equation 11

For $n > 1$, differentiating eq 11 twice with respect to q at constant temperature results in the following equations:

$$\frac{d\Delta H_s}{dq} = -\frac{E}{n} \frac{1}{q} \left(\ln \frac{q_0}{q} \right)^{1/n-1} + \frac{\alpha TE}{n} \frac{(n-1)}{n} \frac{1}{q} \left(\ln \frac{q_0}{q} \right)^{1/n-2} \quad (\text{C-1})$$

and

$$\frac{d^2\Delta H_s}{dq^2} = \frac{1}{q^2} \left[\frac{E}{n} \left(\ln \frac{q_0}{q} \right)^{1/n-1} - \frac{\alpha TE}{n} \frac{(n-1)}{n} \frac{1}{q} \left(\ln \frac{q_0}{q} \right)^{1/n-2} \right] + \frac{1}{q^2} \frac{E}{n} \frac{(n-1)}{n} \left[-\left(\ln \frac{q_0}{q} \right) + \frac{\alpha T(2n-1)}{n} \right] \left(\ln \frac{q_0}{q} \right)^{1/n-3} \quad (\text{C-2})$$

Equation C-1 is set equal to zero:

$$-\frac{E}{n} \frac{1}{q} \left(\ln \frac{q_0}{q_p} \right)^{1/n-1} + \frac{\alpha TE}{n} \frac{(n-1)}{n} \frac{1}{q} \left(\ln \frac{q_0}{q_p} \right)^{1/n-2} = 0 \quad (\text{C-3})$$

Solving eq C-3 for q_p/q_0 yields

$$\frac{q_p}{q_0} = e^{-\alpha T(n-1)/n} \quad (\text{C-4})$$

For $n > 1$, the isosteric heat of adsorption, ΔH_s , reaches its minimum ($\Delta H_{s,\min}$) at $q = q_p$, since substituting eqs C-3 and C-4 into eq C-2 gives

$$\frac{d^2\Delta H_s}{dq^2} \Big|_{q=q_p} = \frac{1}{q_p^2} \frac{\alpha TE}{n} \frac{(n-1)}{n} \left(\frac{\alpha T(n-1)}{n} \right)^{1/n-3} > 0 \quad (\text{C-5})$$

Subsequently substituting eq C-4 into eq 11 yields

$$\Delta H_{s,\min} = \frac{RT^2}{P_0} \frac{dP_0}{dT} + E \left(\frac{\alpha T}{n} \right)^{1/n-1} \quad (\text{C-6})$$

Literature Cited

- Yang, R. T. *Gas Separation by Adsorption Processes*; Brenner, H., Ed.; Butterworth Publishers: Stoneham, MA, 1987; 352 pp.
- Do, D. D. *Adsorption Analysis: Equilibria and Kinetics*; Series on Chemical Engineering Vol. 2; Imperial College Press: Singapore, 1998; 892 pp.
- Sullivan, P. D.; Rood, M. J.; Hay, K. J.; Qi, S. Adsorption and electrothermal desorption of hazardous organic vapors. *J. Environ. Eng.* **2001**, *127* (3), 217–223.
- Sullivan, P. D.; Rood, M. J.; Grevillot, G.; Wander, J. D.; Hay, K. J. Activated carbon fiber cloth electrothermal swing adsorption system. *Environ. Sci. Technol.* **2004**, *38* (18), 4865–4877.
- Dombrowski, K. D.; Lehmann, C. M. B.; Sullivan, P. D.; Ramirez, D.; Rood, M. J.; Hay, K. J. Solvent recovery and energy efficiency during electric regeneration of an ACF adsorber. *J. Environ. Eng.* **2004**, *130* (3), 268–275.
- Talu, O.; Kabel, R. L. Isosteric heat of adsorption and the vacancy solution model. *AIChE J.* **1987**, *33* (3), 510–514.
- Rozwadowski, M.; Siedlewski, J.; Wojzs, R. Sorption of polar substances on active carbons. *Carbon* **1979**, *17* (5), 411–417.
- Stoeckli, F.; Lopez-Ramon, M. V.; Hugi-Cleary, D.; Guillot, A. Micropore sizes in activated carbons determined from the Dubinin–Radushkevich equation. *Carbon* **2001**, *39* (7), 1115–1116.
- Dubinin, M. M. *Progress in Surface and Membrane Science*, Vol. 9; Cadenhead, D. A., Danielli, J. F., Rosenberg, M. D., Eds.; Academic Press: New York, 1975; 70 pp.
- Khan, A. R.; Attaullah, R.; Al-Haddad, A. Equilibrium gaseous adsorption at different temperatures. *J. Environ. Eng.* **1999**, *125* (6), 548–555.
- Condon, J. B. Equivalency of the Dubinin–Polanyi equations and the QM based sorption isotherm equation. A mathematical derivation. *Microporous Mesoporous Mater.* **2000**, *38* (2–3), 356–376.
- Dubinin, M. M.; Polyakov, N. S.; Kataeva, L. I. Basic properties of equations for physical vapor adsorption in micropores of carbon adsorbents assuming a normal micropore distribution. *Carbon* **1991**, *29* (4/5), 481–488.
- Wood, G. O. Activated carbon adsorption capacities for vapors. *Carbon* **1992**, *30* (4), 593–599.
- Tien, C. *Adsorption Calculations and Modeling*; Butterworth-Heinemann: Stoneham, MA, 1994; 244 pp.
- Adamson, A. W. *Physical Chemistry of Surfaces*; John Wiley & Sons: New York, 1982; 664 pp.
- Al-Muhtaseb, S. A.; Ritter, J. A. Roles of surface heterogeneity and lateral interactions on the isosteric heat of adsorption and adsorbed phase heat capacity. *J. Phys. Chem. B* **1999**, *103* (13), 2467–2479.
- Sircar, S. Estimation of isosteric heats of adsorption of single gas and multicomponent gas mixtures. *Ind. Eng. Chem. Res.* **1992**, *31* (7), 1813–1819.
- Talu, O.; Myers, A. L. Rigorous thermodynamic treatment of gas adsorption. *AIChE J.* **1988**, *34* (11), 1887–1893.
- Reid, R. C.; Prausnitz, J. M.; Poling, B. E. *The Properties of Gases & Liquids*, 4th ed.; Sun, B., Fleck, G. H., Eds.; McGraw-Hill: New York, 1987; 741 pp.
- Lo, S.; Ramirez, D.; Rood, M. J.; Hay, K. J. Characterization of the physical, thermal and adsorption properties of a series of activated carbon fiber cloths. In *Proceedings of A&WMA 95th Annual Conference and Exhibition*, Baltimore, MD, 2002; Paper 43166.
- Ramirez, D.; Sullivan, P. D.; Rood, M. J.; Hay, K. J. Equilibrium adsorption of phenol-, tire- and coal-derived activated carbons for organic vapors. *J. Environ. Eng.* **2004**, *130* (3), 231–241.
- Do, D. D.; Do, H. A. A new adsorption isotherm for heterogeneous adsorbent based on the isosteric heat as a function of loading. *Chem. Eng. Sci.* **1997**, *52* (2), 297–310.
- Lide, D. R., Ed. *Handbook of Chemistry and Physics*, 74th ed.; CRC Press: Boca Raton, FL, 1993.
- Foster, K. L.; Fuerman, R. G.; Economy, J.; Larson, S. M.; Rood, M. J. Adsorption characteristics of trace volatile organic compounds in gas streams onto activated carbon fibers. *Chem. Mater.* **1992**, *4* (5), 1068–1073.
- Lordgooei, M.; Rood, M. J.; Rostam-Abadi, M. Modeling effective diffusivity of volatile organic compounds in activated carbon fiber. *Environ. Sci. Technol.* **2001**, *35* (3), 613–619.
- Wang, Z. M.; Kaneko, K. Dipole oriented states of SO_2 confined in a slit-shaped graphitic subnanospace from calorimetry. *J. Phys. Chem.* **1995**, *99* (45), 16714–16721.
- Aittomaki, A.; Viita, I.; Valimaki, A. Isothermal calorimeter for measuring heat of adsorption. *Exp. Therm. Fluid Sci.* **1992**, *5* (4), 570–573.
- He, Y.; Yun, J.-H.; Seaton, N. A. Adsorption equilibrium of binary methane/ethane mixtures in BPL activated carbon: isotherms and calorimetric heats of adsorption. *Langmuir* **2004**, *20* (16), 6668–6678.

Received for review November 25, 2004. Revised manuscript received May 5, 2005. Accepted May 13, 2005.

ES048144R